

Ecological patterns and adaptability of bacterial communities in alkaline copper mine drainage

Jinxian Liu ^a, Cui Li ^b, Juhui Jing ^c, Pengyu Zhao ^a, Zhengming Luo ^a, Miaowen Cao ^a, Zhuanzhuan Ma ^c, Tong Jia ^a, Baofeng Chai ^{a,*}

^a Institute of Loess Plateau, Shanxi University, Taiyuan, 030006, China

^b Faculty of Environment Economics, Shanxi University of Finance and Economics, Taiyuan, 030006, China

^c Institute of Biotechnology, Shanxi University, Taiyuan, 030006, China

ARTICLE INFO

Article history:

Received 7 November 2017

Received in revised form

31 December 2017

Accepted 5 January 2018

Available online 9 January 2018

Keywords:

Bacterial community

Core taxa

NirS

NirK

NosZ_I

qPCR

ABSTRACT

Environmental gradient have strong effects on community assembly processes. In order to reveal the effects of alkaline mine drainage (AlkMD) on bacterial and denitrifying bacterial community compositions and diversity in tailings reservoir, here we conducted an experiment to examine all and core bacterial taxa and denitrifying functional genes's (*nirS*, *nirK*, *nosZ_I*) abundance along a chemical gradient in tailings water in Shibahe copper tailings in Zhongtiaoshan, China. Differences in bacterial and denitrifying bacterial community compositions in different habitats and their relationships with environmental parameters were analyzed. The results showed that the richness and diversity of bacterial community in downstream seeping water (SDSW) were the largest, while that in upstream tailings water (STW1) were the lowest. The diversity and abundance of bacterial communities tended to increase from STW1 to SDSW. The variation of bacterial community diversity was significantly related to electro-conductivity (EC), nitrate (NO₃⁻), nitrite (NO₂⁻), total carbon (TC), inorganic carbon (IC) and sulfate (SO₄²⁻), but was not correlated with geographic distance in local scale. Core taxa from class to genus were all significantly related to NO₃⁻ and NO₂⁻. Core taxa *Rhodobacteraceae*, *Rhodobacter*, *Acinetobacter* and *Hydrogenophaga* were typical denitrifying bacteria. The variation trends of these groups were consistent with the copy number of *nirS*, *nirK* and *nosZ_I*, demonstrating their importance in the process of nitrogen reduction. The copy number of *nirK*, *nosZ_I* and *nirS/16S* rDNA, *nirK/16S* DNA correlated strongly with NO₃⁻, NO₂⁻ and IC, but *nirS* and *nosZ_I/16S*rDNA had no significant correlation with NO₃⁻ and NO₂⁻. The copy numbers of denitrifying functional genes (*nirS*, *nirK* and *nosZ_I*) were negatively correlated with heavy metal plumbum (Pb) and zinc (Zn). It showed that heavy metal contamination was an important factor affecting the structure of denitrifying bacterial community in AlkMD. In this study we have identified the distribution pattern of bacterial community along physiochemical gradients in alkaline tailings reservoir and displayed the driving force of shaping the structure of bacterial community. The influence of NO₃⁻, NO₂⁻, IC and heavy metal Pb and Zn on bacterial community might via their influence on the functional groups involving nitrogen, carbon and metal metabolisms.

© 2018 Elsevier Ltd. All rights reserved.

1. Introduction

Microbial diversity, abundance and community composition change along environmental gradients (Bier et al., 2015; Fan et al., 2016), and these changes may help us identify a set of environmental characteristics to some groups of taxa. The main purpose to

determine the mechanisms of community adaptability is explaining the variation of ecosystem functioning, ultimately, predicting ecosystem responses to current and future environmental changes. Functional genes, which contain the genes encoding key enzymes involved in biogeochemical cycling processes, have been used to study microbial communities (Xu et al., 2010). The abundance of microbial functional genes reflects the adaptability of functional groups in a specific ecological system. So establishing the connection between community structure and function has been a main goal in microbial ecology (Berlemont et al., 2014). At the same time,

* Corresponding author.

E-mail address: bfchai@sxu.edu.cn (B. Chai).

establishing such a connection is especially critical for predicting how communities and functions will respond to environmental change (Trivedi et al., 2013).

Shifts in the abundance and community composition contributing to a process represent another route by which an ecosystem can respond to environmental change (Allison et al., 2013). Bacterial diversity, abundance and functional genes shift considerably along gradients of pH (Kuang et al., 2016), available energy (Gülay et al., 2016; Guo et al., 2015), trace metal concentration (Kumari et al., 2015; Sun et al., 2016), salinity (Dini-Andreote et al., 2014) and temperature (Zhou et al., 2016). Environmental change acts as a selective force against sensitive individuals, resulting in species losses and possible cascading effects on ecosystem function (Carlisle and Clements 2005). Because the composition and functional genes abundance of microbial communities can be affected strongly by pH, salinity, metal concentrations and available energy, we speculated that exposure to alkaline copper mine drainage (AlkMD) would drive the shifts in microbial communities and specific functional groups composition.

Nitrogen contamination in tailings reservoir is mainly caused by the blast of ammonium nitrate, fuel oil explosives, cyanide destruction, flotation agent and the leaching or erosion of rain-water. The excessive nitrogen is mainly removed by microbial denitrification in tailings water. Denitrification is an important microbial process that removes excessive nitrogen from contaminated water. This dissimilatory process reduces nitrate (NO_3^-) to nitrogen gas (N_2) through intermediates of nitrite (NO_2^-), nitric oxide (NO) and nitrous oxide (N_2O). It is well known that the denitrification process exists in multiple environments: wastewater (Gonzalez-Martinez et al., 2015; Xing et al., 2017), grassland soil (Harter et al., 2014; Pan et al., 2016), lakes, agricultural fields (Ai et al., 2017; Ishii et al., 2011), sediments (Baeseman et al., 2006). However, at present, there is no report on the denitrifying bacteria in AlkMD. As bacteria play a central role in denitrification, it is crucial to understand which factors control the abundance of denitrifying functional genes in AlkMD.

Zhongtiaoshan copper mine is the largest non-coal underground mining mine in China, with annual output of more than 4 million tons of ore (Liu et al., 2017). It has a copper-dominated ore body and is accompanied by some other metals such as Fe, Pb, Zn, Cd, Mo et al. (He et al., 2007). Large amounts of waste water and waste residue containing a variety of heavy metals are produced in the process of mining. Massive accumulations of tailings cause

serious pollution to the ecological environment, so ecological restoration is particularly important in this region. Microorganisms play an important role in the process of ecological restoration, which can reduce the toxicity of heavy metals and decompose excessive nutrient elements in tailings water. The structure and diversity of microbial communities and the structure of functional microbial communities determine the resilience of the ecosystem.

This study aimed to address the following questions: (i) How does AlkMD affect microbial community structure? (ii) How does AlkMD affect core taxa? (iii) How does AlkMD affect microbial functional gene abundance? Our results indicated that microbial community composition and functional gene structure were distinct among sampling sites. Moreover, such microbial functional patterns were highly correlated to environmental factors. We speculate that the community structure in AlkMD was shaped by environmental factors via influence on the functional microbial groups.

2. Materials and methods

2.1. Site description

Sampling sites are in Shibahe tailings reservoir ($35^{\circ}15' \sim 35^{\circ}17' \text{N}$, $111^{\circ}38' \sim 111^{\circ}39' \text{E}$), 10 km away from the Zhongtiaoshan copper base, which lies in the south of Shanxi province, China. This tailings reservoir has been used since 1972, with an area of 2 million square meters, the maximum storage capacity of 125 million cubic meters, the current capacity of 100 million cubic meters, and the average depth of 5 m in the catchment area. The research area belongs to continental monsoon climate, with an annual mean temperature of 14°C , an annual precipitation around 780 mm and frost free period is more than 200 days. Two seeping water samples (SUSW and SDSW) and three tailings water samples (STW1, STW2 and STW3) were selected (Fig. 1).

2.2. Sampling procedures

Water samples were collected at the same depth (~1m from water surface) using automatic sampler (W2BC-9600) in September 2016. Three replicates were taken at each sampling point and each repeat took 2 L water. Microbial mass was *in situ* harvested from 1.5 L water sample, using a sterile $0.2 \mu\text{m}$ pore size (Millipore, Jinteng, Tianjin, China) membrane filter. The millipore

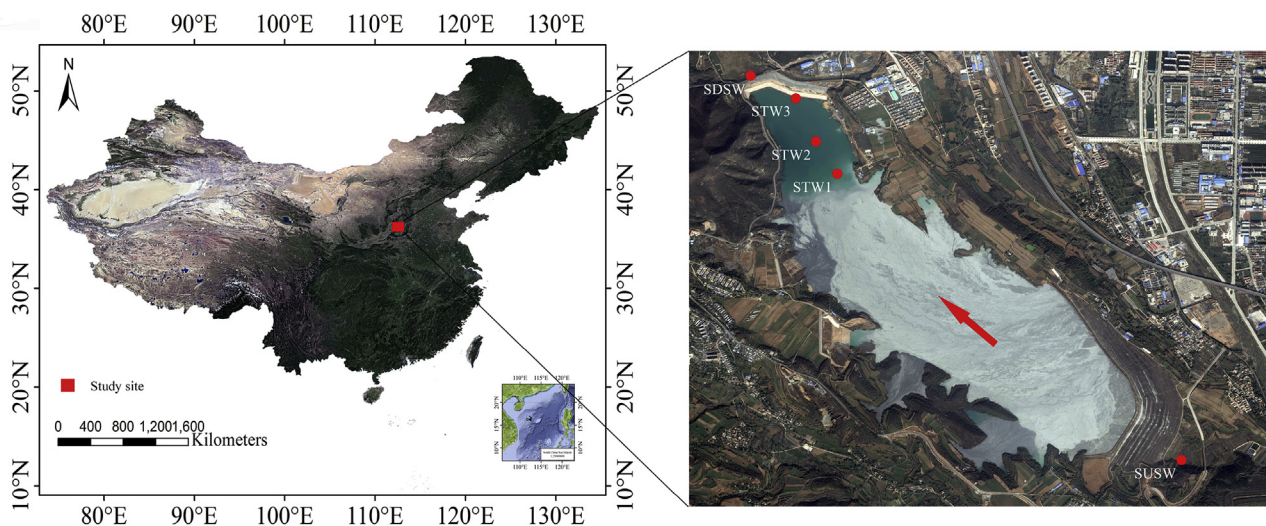


Fig. 1. Locations of sampling sites around the Shibahe tailings reservoir in Shanxi province, China. Arrow shows flow direction of tailings water.

filter with microbes used for microbial DNA extraction was sealed at the sterile centrifuge tube and then stored in portable liquid nitrogen tank. The remaining 0.5 L water was used for physico-chemical property analysis.

2.3. Physicochemical analysis

Water physicochemical properties were measured at each site. The pH, dissolved oxygen (DO), conductivity (EC), nitrate (NO_3^-) and ammonium (NH_4^+) content were measured *in situ* by a portable water quality monitor (Aquaread AP-2000, UK); total carbon (TC), total organic carbon (TOC) and inorganic carbon (IC) content were measured by a TOC analyzer (Shimadzu, TOC-V_{CPH}, Japan); nitrite (NO_2^-) and sulfate (SO_4^{2-}) content were measured by an automated discrete analyzer (DeChem-Tech, CleverChem380, Germany); concentrations of heavy metals (As, Cd, Cu, Pb, Zn) content were determined by ICP-AES (iCAP 6000, Thermo Fisher, UK).

2.4. DNA extractions, PCR amplification and high-throughput sequencing

Biomass-sticking filters were cut into pieces and placed into centrifuge tubes for DNA extraction using a Fast DNA SPIN extraction kits (MP Biomedicals, Santa Ana, CA, USA), according to the manufacturer's protocol. A total of five samples (mixing the three repeats for a sample) were analyzed for bacteria communities. The primer pair 338F (5'-ACTCCTACGGGAG GCAGCA-3') and 806R (5'-GGACTACHVGGGTWCTAAT-3') were used to amplify the V3-V4 hyper variable region of 16S rDNA gene in bacteria. Each sample was amplified in triplicate with 25 μL reactions under the following procedure: 98 °C for 2 min (initial denaturation), 26 cycles of 15 s at 98 °C (denaturation), 55 °C for 30s (annealing), and 72 °C for 30s (extension), followed by 5 min at 72 °C. Triplicate of PCR products were pooled together and purified by the Agarose Gel DNA purification kit (TIANGEN, China) and quantified with the NanoDrop device. Samples were run on an Illumina MiSeq platform according to the manufacturer's instruction manual. High-throughput sequencing analysis and bioinformatics analysis were described in the supplementary material. The sequencing and bioinformatics service were conducted by Shanghai Personal Biotechnology co., LTD.

2.5. Nucleic acid sequences

The raw sequence data of bacterial 16S rDNA genes has been deposited into the NCBI GenBank under the study accession number SRP116887.

2.6. Real time q-PCR assays

Four target genes were quantified, including 16S rDNA of total bacterial, and three denitrifying bacterial genes (*nirS*, *nirK* and *nosZ*). All q-PCR assays were performed in triplicates by using a CFX96 system (BioRad, USA). The template DNA concentrations and plasmid DNA concentrations were quantified by using Infinite M200 PRO (Tecan, Switzerland) and the DNA concentration of each sample was adjusted to yield a concentration of 10 ng μL^{-1} . For q-PCR quantification of the 16S rDNA, *nirS*, *nirK*, and *nosZ* genes primers selected were listed in supplementary material (Table S1). Each reaction mixture contained 10 μL of SYBR[®] Premix Ex Taq[™] (Tli RNaseH Plus) (TaKaRa, Dalian, China), 0.5 μL of each primer (10 $\mu\text{mol L}^{-1}$) for the selected target gene (except for 16S rDNA 1 μL of each primer), 5 μL of DNA (except for 16S rDNA 1 μL), and double distilled water to yield a total volume of 20 μL . The PCR procedure for 16S rDNA included an initial denaturation step at

95 °C for 3 min and 40 cycles of amplification (95 °C for 20s, 55 °C for 30s and 72 °C for 30 s). Finally, an increase of 0.5 °C⁻¹ from 65 to 95 was performed to obtain the melting curve analysis of PCR products. The thermal cycling conditions for other genes were the same as the one described before, except that the annealing temperature was 58 °C for *nirS* and *nosZ*, 62 °C for *nirK*.

Target gene copy numbers in samples were calculated from the standard curves. Standard curves were constructed from PCR amplicons products of the target gene fragments extracted from agarose gel with a Gel Extraction Kit (TIANGEN, China). The purified product was connected with pMD[®]18-T plasmid vector (Takara Bio, Dalian), and transformed into competent *Escherichia coli* DH5 α cells. The transformant cells were plated on agar plates supplemented with 1 mL AMP, 5 mL IPTG and 0.8 mL X-Gal every liter Luria-Bertani (LB) and incubated in 37 °C. Positive clones were subcultured to fresh LB. Then the plasmids were extracted from the correct insert clones for each target gene and then were used as standards for quantitative analyses. Tenfold serial dilutions of the known copies of the plasmid DNA were then subjected to quantitative PCR in triplicate to generate an external standard curve. A dilution series of 10⁸ -10³ gene copies were used as standards in each qPCR run. Efficiencies for PCR reactions were 81.3% for *nirS*, 79% for *nirK*, 86.8% for *nosZ*, and 101.1% for 16S rDNA.

2.7. Data analysis

Data were square root- or log-transformed, where necessary to improve normality and reduce heteroscedasticity before analysis. Statistical differences among the sampling points of environmental parameters, copy numbers of 16S rDNA, *nirS*, *nirK*, *nosZ*, and ratios of *nirS*/16S rDNA, *nirK*/16S rDNA and *nosZ*/16S rDNA were analyzed by one-way ANOVA, besides Kruskal Wallis significance difference (KW) test was used for multiple comparison. Principal coordinate analysis (PCoA) using Bray-Curtis distance was used to estimate the differences of community structure between samples. Mantel test was performed to assess the correlations between bacterial community structure and environmental parameters. Multiple-correlation analyses making use of Pearson's method were used to relate all bacterial and denitrifying bacterial abundances and relative abundance of core taxa and denitrifying bacteria with environmental parameters. Redundancy analysis (RDA) was used to identify the linkages between core taxa and environmental variables. Confidence interval of 95% ($p < .05$) was used, statistical analyses were performed using software SPSS 20.0 (IBM SPSS statistics, USA), Canoco (version 5.0, USA) and PAST (version 3.15).

3. Results

3.1. The physicochemical gradient of drainage in tailings reservoir

Sampling locations spanned a gradient of AlkMD contamination. The highest values of pH, NO_3^- , NO_2^- were observed at STW1, which were significantly higher than that of STW3, SDSW and SUSW (Table 1). The pH, EC, NO_3^- , NO_2^- and SO_4^{2-} showed a gradient along flow direction of drainage water that were STW1>STW2>STW3. As the tailings dam was built by the accretion of tailings sand, just like a filter column, part of the heavy metals and other contaminants were filtered out when the drainage permeates the tailings dam. Therefore, seeping water in SUSW and SDSW had lower pH, EC, NO_3^- , NO_2^- and SO_4^{2-} compared with STW water.

The higher levels of DO, TC, TOC, and IC were measured at STW3, showing a trend of increase (STW1<STW2<STW3) along the flow direction of drainage water (Table 1). EC, SO_4^{2-} , NH_4^+ , TC and TOC, had significant difference in SUSW and SDSW. For these five heavy metals monitored, only Cd and Zn gradually decreased along the

Table 1
Average water physical and chemical values of five sampling points.

Factors	STW1	STW2	STW3	SUSW	SDSW
	Mean ± SE	Mean ± SE	Mean ± SE	Mean ± SE	Mean ± SE
pH	9.382 ± 0.095a	9.131 ± 0.053a	8.147 ± 0.048b	8.190 ± 0.032b	8.014 ± 0.076b
DO	8.560 ± 0.195a	10.218 ± 0.466a	10.661 ± 0.527a	10.643 ± 0.281a	11.114 ± 3.292a
EC	1834.333 ± 31.205a	1832.001 ± 20.466a	865.143 ± 3.106b	1427.333 ± 59.218 ab	404.333 ± 8.511c
NO ₃ ⁻	134.373 ± 5.417a	85.170 ± 1.553 ab	14.315 ± 1.142bc	5.265 ± 0.345c	4.698 ± 0.364c
NO ₂ ⁻	10.548 ± 0.405a	6.959 ± 0.20 ab	1.259 ± 0.096bc	0.575 ± 0.057c	0.478 ± 0.044c
NH ₄ ⁺	1.453 ± 0.003 ab	1.715 ± 0.019a	0.340 ± 0.116b	2.333 ± 0.030a	0.387 ± 0.015b
TC	20.600 ± 0.035c	24.723 ± 0.818bc	34.523 ± 3.215 ab	25.070 ± 0.023bc	52.315 ± 0.136a
TOC	7.597 ± 0.003abc	8.520 ± 1.529bc	14.100 ± 0.075 ab	5.253 ± 0.020c	19.344 ± 3.374a
IC	13.005 ± 0.032c	16.202 ± 0.291bc	20.179 ± 2.703bc	19.820 ± 0.001 ab	43.015 ± 0.061a
SO ₄ ²⁻	1582.500 ± 2.977a	1207.558 ± 100.997a	837.255 ± 38.754 ab	897.900 ± 97.900 ab	117.655 ± 11.311c
As	2.407 ± 0.021a	2.853 ± 0.171 a	0.155 ± 0.012b	0.180 ± 0.009 ab	0.003 ± 0.003b
Cd	0.004 ± 0.001a	0.002 ± 0.001a	0.002 ± 0.003a	0.003 ± 0.002a	BDL
Cu	0.017 ± 0.009 ab	0.032 ± 0.004a	0.016 ± 0.004 ab	0.006 ± 0.002b	0.008 ± 0.001b
Pb	0.060 ± 0.036a	0.021 ± 0.013a	0.025 ± 0.030a	0.043 ± 0.006a	BDL
Zn	0.012 ± 0.001 ab	0.011 ± 0.004b	0.009 ± 0.003b	2.741 ± 1.058a	0.249 ± 0.057a

Abbreviations : pH has no unit of measurement; EC unit is uS/cm; the unit of others is mg·L⁻¹; BDL indicate below detection level. Different letters represent significant differences in $P < .05$ level between different samples.

flow direction, but there was no significant difference among three drainage water sample points.

3.2. Overall bacterial community structure and taxa identification

Most of the filtered reads were within 400–500 bp in length, averagely longer than 400 bp. In total, 27587, 28168, 23429, 22330 and 21077 filtered sequences were obtained in five samples, respectively. According to sequence alignment at a sequence identity cut-off value of 97%, 370, 687, 905, 685 and 1010 OTUs were identified correspondingly (Table 2).

According to the α -diversity analysis, the Shannon values indicating the microbial diversity in five sample points were 3.16, 5.79, 5.65, 5.39 and 6.37, respectively, demonstrating a higher microbial diversity in four samples (SUSW, STW2, STW3, SDSW) compared with that in STW1. The OTUs, ACE, Chao1 and Simpson indices were all minimal in STW1 compare to the other four samples, and bacterial community richness showed an increasing trend along the direction of the flow (Table 2).

PCoA based on Bray-Curtis similarities showed that microbial community structures at different sampling locations were different. Microbial communities of five sampling points were divided into three groups with obvious differences in STW1, STW2 and SUSW, STW3 and SDSW (Fig. 2). The similarities of bacterial community structures were matched with the physicochemical properties of drainage water samples (Table 1).

Approximately 99.9% of the sequences were classified into 26 different phyla across all the samples (Fig. 3). The predominant phyla (relative abundance was greater than 1%) were *Proteobacteria* (the number of classified sequences in this phylum ranged from 41.20 to 89.49% in all the samples), *Actinobacteria* (0.41–24.44%), [*Thermi*] (2.30–22.81%), *Firmicutes* (3.79–13.99%), *Bacteroidetes* (2.50–7.72%), *Cyanobacteria* (0.11–4.70%), *Chloroflexi* (0.004–1.51%), *Verrucomicrobia* (0.01–2.19%) and *OD1* (0.007–1.30%). There were

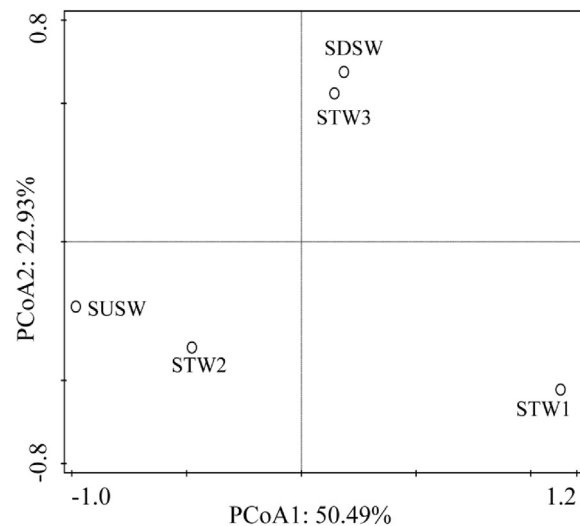


Fig. 2. Principal co-ordinates analysis based on Bray-Curtis similarities of bacterial communities found at the five sample points.

seven predominant phyla which had significant correlation with environmental parameters (Table S3). *Proteobacteria* in the five samples was distributed across the alpha (21.44–76.15%), beta (2.49–12.31%) and gamma (1.03–38.81%) subphyla, however, delta (0.005–0.35%) subphyla were detected in four samples except STW1. Sequencing data showed that the composition of taxa in five samples was different.

There were a large proportion of sequences (31.80–66.70%) which were not assigned to any genera. Bacterial communities in STW1 were dominated (54.06%) by sequences of an uncultured genus of the *Rhodobacteraceae*. The abundance of *Rhodobacteraceae*

Table 2
Phylotype richness and diversity estimators of the bacterial communities in five sampling points.

Sampling point	High quality sequence	OTUs	ACE	Chao1	Shannon	Simpson
STW1	27587	370	334.61	238.00	3.16	0.70
STW2	28168	687	606.46	459.00	5.79	0.96
STW3	23429	905	885.96	650.00	5.65	0.88
SUSW	22330	685	607.93	467.00	5.39	0.93
SDSW	21077	1010	734.00	734.00	6.37	0.95

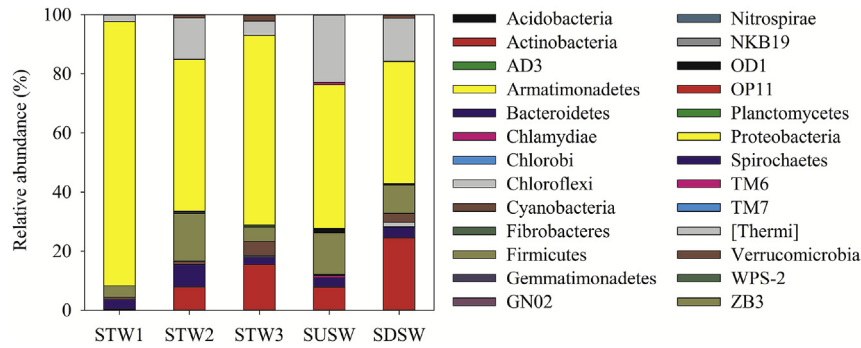


Fig. 3. Bacterial community structure of each sampling point at the phyla level.

gradually decreased along the direction of flow. The most abundant bacteria was *Deinococcus* (class *Deinococci*) in STW2 (13.92%) and SUSW (22.81%), *Acinetobacter* (class γ -proteobacterial) in STW3 (37.76%) and *Mycobacterium* (class *Actinobacteria*) in SDSW (15.86%) (Fig. 5, Table S2).

Bacterial abundances, expressed gene copies in per mL water, were based on broad 16S rDNA targeted q-PCR were ranging from $6.90 \times 10^5 \pm 5.45 \times 10^4$ (STW1) to $5.14 \times 10^6 \pm 3.40 \times 10^5$ (SDSW) of total bacteria. The bacterial 16S rDNA gene copy number was significantly different ($P < .01$) among five samples (Fig. 4), and this difference was correlated positively with DO, TC, TOC and IC and negatively with EC, NO_3^- , NO_2^- , NH_4^+ , SO_4^{2-} , As and Pb (Table 4).

3.3. Spatial patterns of core taxa

The top ten taxa with relative abundance greater than 1% (at the level of class, order, family and genus, respectively) were defined as core taxa. Top ten classes accounted for 90.6–97.9% of the total identified sequences (Fig. 5a), top ten orders accounted for 82.2–92.0% (Fig. 5b), top ten families accounted for 62.1–86.7% (Fig. 5c) and top ten genera represented 27.3–56.4% (Fig. 5d).

There was considerable inconsistency among five samples. The relative abundance of *Alphaproteobacteria* (order *Rhodobacteriales*, family *Rhodobacteraceae* and genus *Rhodobacter*) and *Betaproteobacteria* (order *Burkholderiales*, family *Comamonadaceae* and genus *Hydrogenophaga*) gradually decreased along flow direction of

drainage water. However, *Gammaproteobacteria* (order *Pseudomonadales*, family *Moraxellaceae*, genus *Acinetobacter* and *Legionella*); *Actinobacteria* (order *Actinomycetales*, family *Mycobacteriaceae* and genus *Mycobacterium*); *Synechococcophycideae* (genus *Synechococcus*); *Acidimicrobiia*; *Caulobacteriales* (family *Caulobacteraceae*) and *Rhizobiales* (family *Phyllobacteriaceae*) gradually increased along flow direction of drainage water (Fig. 5).

The highest relative abundance of *Deinococci* (order *Deinococcales*, family *Deinococcaceae* and genus *Deinococcus*), *Bacilli* (order *Bacillales*, family *Bacillaceae* and genus *Bacillus*), *Flavobacteriia* (order *Flavobacteriales*), *Sphingomonadales* (family *Sphingomonadaceae* and genus *Novosphingobium*), *Sphingobacteriia* and *Microbacteriaceae* (genus *Candidatus Aquiluna*) were observed in the STW2. There were also differences of core taxa community structure in SUSW and SDSW (Fig. 5).

3.4. Relationships of bacterial community composition and environmental parameters

Mantel test showed that total bacterial community composition (all OTUs) was strongly correlated with EC, NO_3^- , NO_2^- , TC and SO_4^{2-} ; likewise, the predominant bacterial community composition (abundant OTUs) was significantly correlated to EC, NO_3^- , NO_2^- and IC (Table 3). In addition, mantel tests also showed that the total and predominant bacterial community composition were not significantly correlated with pH, DO, heavy metal (As, Cd, Cu, Pb, Zn) and geographic distance (Table 3).

RDA analysis results showed environmental parameters had significant influence on core taxa at the level of class ($F = 2.4$, $P < .05$), order ($F = 2.6$, $P < .05$), family ($F = 2.5$, $P < .05$) and genus ($F = 7.1$, $P < .05$). The results showed that core taxa were closely related to the content of NO_3^- and NO_2^- , also SO_4^{2-} showed a significant influence on the class, order and family level and pH on the order and family level (Table S8). Multiple correlation analysis results showed that NO_3^- , NO_2^- , TC, IC, SO_4^{2-} and heavy metal (As, Cu, Pb, Zn) had significant influence in several core taxa (Tables S3–S7).

3.5. Variations of *nirS*, *nirK* and *nosZ_I* along drainage flow direction

Key functional genes for denitrification comprising genes encoding nitrite reductase (*nirS* and *nirK*) and nitrous oxide reductase (*nosZ_I*) were detected in five samples. The *nirS*, *nirK* and *nosZ_I* gene copy numbers ranged from 2.12×10^3 to 3.23×10^4 , 4.73×10^0 to 3.84×10^4 and 4.14×10^4 to 2.33×10^5 copies per mL water, respectively, in the studied samples (Fig. 6). The copy number of *nirS* in STW3 and STW2 were significantly higher than that in STW1, and the copy number of *nirK* did not have significant difference in three reservoir water sampling points. The maximum copy number of *nosZ_I* was observed in STW2, and had significant

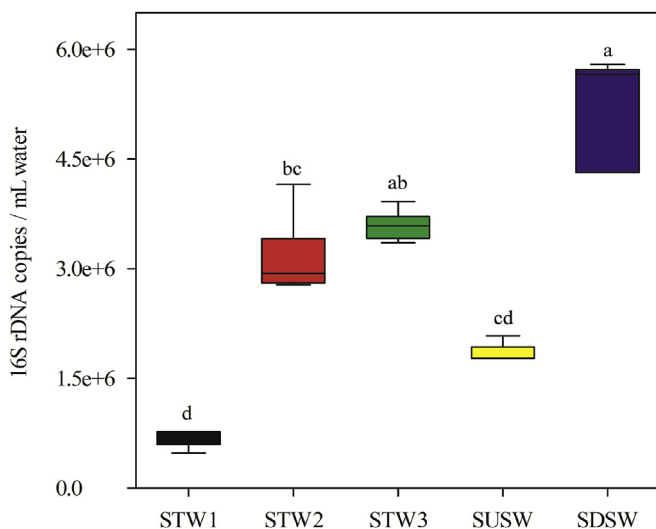


Fig. 4. The distribution pattern of bacterial 16S rDNA copy numbers at the five sample points. Different letters represent significant differences in $P < .05$ level.

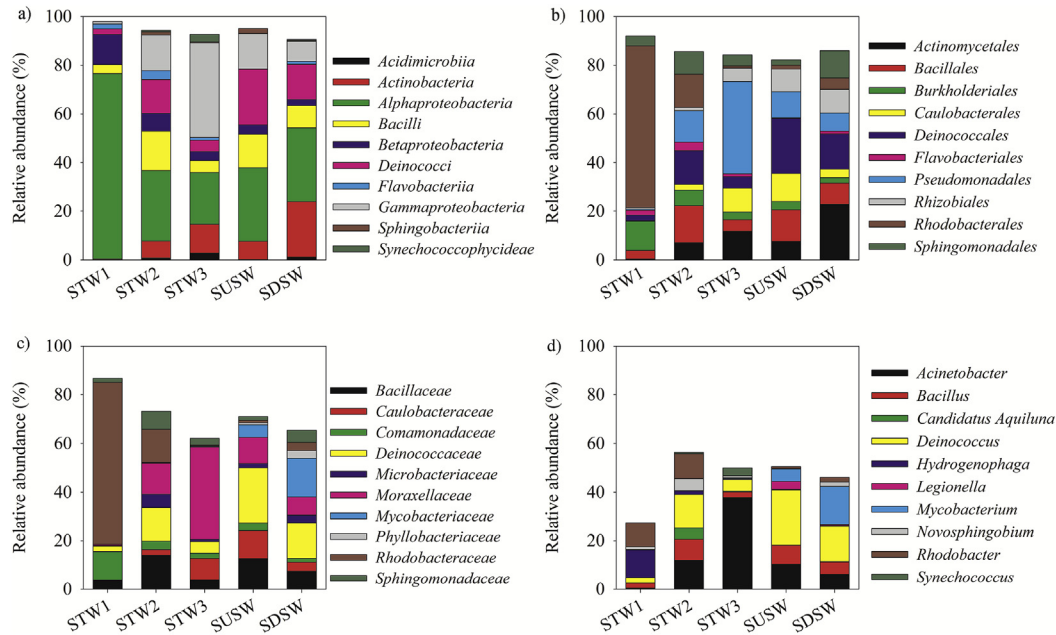


Fig. 5. Core taxa of bacteria in five sampling points. a) Class level; b) Order level; c) Family level; d) Genus level. Core taxa: the top 10 taxa with relative abundance greater than 1% (at the level of class, order, family and genus, respectively).

Table 3

Mantel test showing the correlation between bacterial community dissimilarity and environment parameters in this study.

Factor	All OTUs	Abundant OTUs
pH	0.603	0.822
DO	0.117	-0.188
EC	0.742*	0.595*
NO ₃ ⁻	0.905**	0.596*
NO ₂ ⁻	0.903**	-0.611*
NH ₄ ⁺	0.151	-0.012
TC	0.558*	-0.012
TOC	0.303	-0.130
IC	0.398	0.367*
SO ₄ ²⁻	0.679*	0.132
As	0.621	-0.161
Cd	0.268	-0.372
Cu	0.150	0.602
Pb	-0.432	-0.257
Zn	-0.611	0.851
Geographic distance	0.215	0.620

Abbreviations: pH has no unit of measurement; EC unit is uS/cm; the unit of others is mg·L⁻¹.

The Pearson's coefficients were calculated and their significances were tested based on 999 permutations.

* $P < .05$ and ** $P < .01$. Abundant OTUs: with relative abundance more than 1%.

difference in three reservoir water sampling points. The copy number of three denitrification functional genes in SUSW was significantly lower than in SDSW (Fig. 6).

The ratio of *nirS*/16S rDNA, *nirK*/16S rDNA and *nosZ*_I/16S rDNA ranged from 0.12 to 1.46%, 2.58 to 1.38% and 1.81–6.03% in five sampling points, respectively (Fig. 7). The relative abundance of *nirS*, *nirK* and *nosZ*_I gradual decreased along the direction flow in reservoir water, although there was no statistical significance for *nirS* and *nirK* (Fig. 7). The relative abundance of *nirS*, *nirK* and *nosZ*_I had no significant difference in seeping water. *NirS*/16S rDNA and *nirK*/16S rDNA in reservoir water was 3.71 and 3.49×10^3 times as much as in seeping water, respectively, while *nosZ*_I/16S rDNA in seeping water was 1.22 times as much as in reservoir water.

3.6. The effects of environmental parameters on *nirS*, *nirK* and *nosZ*_I

Denitrifying functional genes *nirS* and *nirK* have similar response strategies to environmental change (except DO), while *nosZ*_I was different. The abundance of *nirS* and *nirK* was positively correlated with pH, NO₃⁻, NO₂⁻, and negatively correlated with IC and Zn, although the effects of nitrogen (NO₃⁻, NO₂⁻) and pH were not statistically significant on *nirS*. However, *nosZ*_I had an opposite trend with *nirS* and *nirK* (Table 4). The abundance of *nirS*, *nirK* and *nosZ*_I were positively correlated with Cu and negatively correlated with Pb (Table 4). The pattern of the relative abundance of three denitrifying genes were consistent across five samples, and all had a negative correlation with sampling location (Fig. 8), which were closely related to the availability of nutrients (NO₃⁻, NO₂⁻, IC), pH and heavy metal (Zn) elements (Table 4).

4. Discussion

4.1. Microbial communities in AlkMD

The distribution of different microbial groups in relation to biotic and abiotic characteristics of its environment can provide important clues to help us to understand the basis of the organism physiology and its function within an ecosystem. Some studies showed that microbial communities were sensitive to changes of local environmental conditions (Mykrä et al., 2017; Nie et al., 2016) and our results were consistent with these previous studies. Our data showed that α -diversity and β -diversity of bacterial community changed along flow direction of drainage (Table 2, Figs. 2 and 4), and these compositional shifts were correlated with the concentration of NO₃⁻, NO₂⁻, SO₄²⁻ and TC (Table 3, Table 4). There was limited evidence showed that such patterns of diversity may be structured by a species-sorting process (i.e., the selection by local environmental conditions) (Crump et al., 2012). This pattern of bacterial community composition was a manifestation of adaptation to environmental conditions such as responses to the availability of nitrate, sulfate and carbon for energy metabolism. Rather, the variation of bacterial abundance might be because of stressors

Table 4

Multiple correlation analysis results showing the correlation with the copy number (16S rDNA, *nirS*, *nirK*, *nosZ_I*), functional gene relative abundances and environment parameters in this study.

Environmental variable	16S rDNA	<i>nirS</i>	<i>nirK</i>	<i>nosZ_I</i>	<i>nirS</i> / 16S rDNA	<i>nirK</i> / 16S rDNA	<i>nosZ_I</i> / 16S rDNA
pH	-0.365	0.256	0.540**	-0.333	0.638***	0.581**	-0.148
DO	0.463*	0.478*	-0.111	0.632***	0.003	-0.219	-0.301
EC	-0.701***	-0.055	0.102	-0.390*	0.432*	0.266	0.070
NO ₃ ⁻	-0.566**	0.111	0.569***	-0.487*	0.674***	0.676***	0.046
NO ₂ ⁻	-0.570**	0.144	0.550**	-0.483*	0.702***	0.659***	0.042
NH ₄ ⁺	-0.609**	-0.367	-0.552**	-0.096	-0.147	-0.354	0.324
TC	0.786***	0.385	-0.152	0.675***	-0.219	-0.359	-0.244
TOC	0.583**	0.602**	0.440*	0.272	0.358	0.247	-0.235
IC	0.565**	-0.591*	-0.586**	0.643***	-0.579**	-0.699***	-0.042
SO ₄ ²⁻	-0.699***	-0.228	0.029	-0.305	0.321	0.240	0.412*
As	-0.457*	-0.084	-0.118	-0.053	0.252	0.000	0.307
Cd	0.061	0.007	0.030	-0.039	0.145	0.021	0.291
Cu	0.080	0.388*	0.156	0.218	0.374	0.113	0.043
Pb	-0.497**	-0.486*	-0.177	-0.416*	-0.053	-0.015	0.487*
Zn	0.016	-0.587**	-0.689***	0.144	-0.725***	-0.625***	0.428*

Note: Values in bold indicate statistical significance. Significance levels are shown at **p* < .05, ***p* < .01 and ****p* < .001.

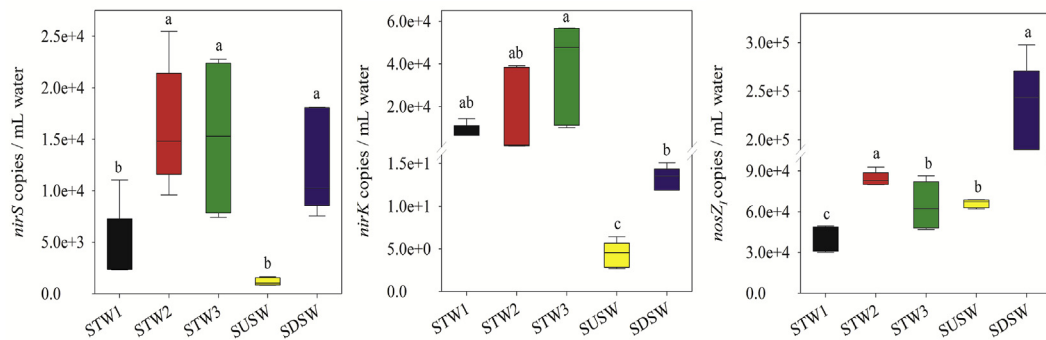


Fig. 6. The copy number of *nirS*, *nirK* and *nosZ_I* at the five sample points. Different letters represent significant differences in *P* < .05 level.

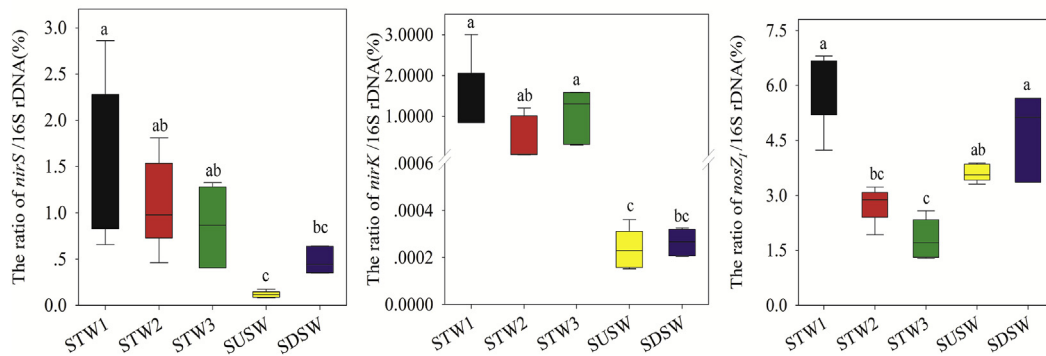


Fig. 7. Abundance of *nirS*, *nirK* and *nosZ_I* genes relative to the amount of 16S rDNA in five sampling points. Different letters represent significant differences in *P* < .05 level.

that effecting cellular processes and signaling (Bier et al., 2015). When an ecosystem exists extreme environmental alteration, such as tailings wastewater discharge, we expect organisms favored by the changes to flourish and sensitive taxa to fail. This stress response could shift community composition across environmental gradients as well as increase taxa richness at lower pollution levels and increase diversity at intermediate pollution levels where sensitive and tolerant taxa overlap (Niyogi et al., 2007). This was a possible explanation for microbial taxa richness and diversity responses to the AlkMD gradient. As and Pb significantly inhibited the abundance of bacterial community (Table 4). Microorganism

community under the action of toxic heavy metals could reduce or even lose the metabolic capability of carbon, nitrogen and sulfur (Li et al., 2015), therefore, high concentrations of heavy metals significantly inhibit the number of bacteria. Heavy metal mediated toxicity was usually due to inactivation of enzymes, membrane impairment, interaction with nucleic acids, variation in nutrient transport and availability of the substrate. The inhibition of enzymes, cell membranes and nucleic acids by heavy metals was due to the binding of metals to enzyme proteins, membrane proteins and nuclease, thereby altering their structure (Yadav et al., 2016), ultimately resulting in the loss of cytoactive. In acid mine drainage

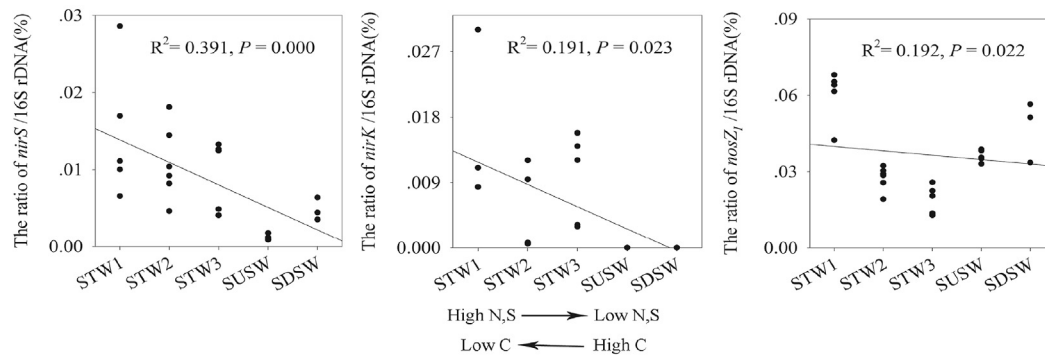


Fig. 8. Correlations between relative abundance of denitrifying functional genes and sampling sites.

(AMD) systems, pH strongly correlates with microbial community diversity, richness and functional gene abundance (Huang et al., 2016; Kuang et al., 2016). Although pH had statistically distinct between reservoir water and seeping water (Table 1), pH was not an important factor correlate of composition or diversity metrics (Table 3, Table 4) in this study. Consistent with prior study on AlkMD (Bier et al., 2015), this might be explained by the limited pH range in this study (8.01–9.38 only 1 orders of magnitude) relative to prior studies in AMD (not less than 4 orders of magnitude). The lack of significant correlation between pH and diversity in Shibahe tailings reservoir suggested that other chemical constituents such as EC, NO_3^- , NO_2^- , SO_4^{2-} and numerous trace elements were stronger determinants of bacterial community structure than pH. Geographical distance had a significant influence on the structure of bacterial community, and the difference of community diversity was obvious with the increase of geographic distance (Lee et al., 2013; Roguet et al., 2015). However, there was no significant correlation between bacterial community structure and geographic distance in this study (Table 3), indicating that the main factor affecting the change of bacterial community structure was environmental selection rather than diffusion limitation. The qPCR estimated all bacterial abundances (Fig. 4) were somewhat higher than those estimated by amplicon sequencing (Table 2), but dissimilarity of bacterial abundance when using different primers (Table S1) in PCR-based surveys was well documented (Gülay et al., 2016). Amplification efficiency of 101.1% for qPCR reactions was also an important factor in overestimation of bacterial abundance.

Bacterial communities assemble because of functional adaptation in extreme habitat (Chan et al., 2013; Kuang et al., 2016). High abundance of a member of the *Proteobacteria* in five samples (Fig. 3), consistent with others of AlkMD (Bier et al., 2015), suggesting their central role in the process of tailings water purification. The largest decrease in abundance from STW1 to SDSW was noted for the *Proteobacteria* due to the decrease of the typical denitrifying taxa (*Rhodobacteraceae*, *Hydrogenophaga* and *Rhodobacter*) (Table S2) resulted from the reduction of NO_3^- and NO_2^- (Table S6, Table S7). The trend of *Actinobacteria* abundance was opposite to *Proteobacteria*, and it gradually increased from STW1 to SDSW (Fig. 3). This was mainly caused by the changes in SO_4^{2-} and TOC concentrations (Table S3) which was consistent with Bier's (Bier et al., 2015) findings on water bacteria. Contrary to this study, Hou (Hou et al., 2017) studied on soil bacteria pointed out that EC was positively related to *Actinobacteria*, whereas TC was negatively related to *Actinobacteria*. This was possibly due to the differences of subjects and study areas. The abundances of *Firmicutes*, *Bacteroidetes* and [*Thermi*] were higher in STW2 and SUSW, which was consistent with the moderate pollution hypothesis, suggesting the three taxa showed similar or slightly different niches (Gülay et al.,

2016). *Cyanobacteria* and *Chloroflexi* were common aquatic autotrophic microorganisms. The relative abundances of *Cyanobacteria* and *Chloroflexi* increased along the flow direction in the reservoir water (Fig. 2). The gradually decrease of NH_4^+ , NO_2^- , NO_3^- and increase of TC concentration (Table S3) were the most important factors affecting the distribution of *Cyanobacteria* and *Chloroflexi*. *Cyanobacteria* adapted contaminated habitats by releasing extracellular polymeric substances buffering against environmental stressors (Flemming et al., 2010). Members of the phylum *Verrucomicrobia* were abundant in diverse habitats, including soil, water, and sediments, as well as extreme environments such as in the hot springs, low pH 2.0–2.5 and soda lake habitats (Freitas et al., 2012; Hou et al., 2008; Shen et al., 2017). The relative abundance of *Verrucomicrobia* increased along the flow direction in reservoir water (Fig. 3), and this could be explained by Pb (Schneider et al., 2017) and TOC (Freitas et al., 2012) concentration change. *OD1* played an important ecological role in impacting hydrogen and sulfur cycles (Castelle et al., 2017; Wrighton et al., 2012). Whether *OD1* is associated with sulfur cycling in AlkMD is pending further study.

4.2. Core taxa and their likely eco-physiology role

The dominant microflora plays a key role in the ecosystem, so the dynamics of the dominant flora can indirectly reflect the adaptation process of the whole bacterial community to environmental change. Ten top core bacterial community composition (from class to genus) varied among the five samples, but core genera were shared across the samples (Fig. 5, Table S2), indicating that environmental conditions in the AlkMD had similar background, and specific conditions of each sample point had secondary influence on the microbial community composition (Gülay et al., 2016). Core taxa (*Rhodobacteraceae*, *Rhodobacter* and *Hydrogenophaga*) in STW1, *Acinetobacter* in STW3, *Deinococcus* in SUSW and *Mycobacterium* in SDSW were abundant (Fig. 5c and d), suggesting different ecological functioning roles. It would indicate selection as a dominant force for community assembly via core taxa of functional microbes.

Core taxa at different taxonomic levels had similar adaptive capabilities, and this adaptation was best explained by NO_3^- , NO_2^- , TC and IC concentration changes (Table S4 - S7). Major aquatic bacteria *Rhodobacteraceae* and alkaliphilic genera *Rhodobacter* were all typical phototrophic purple non-sulfur bacteria and NO_3^- and NO_2^- were used as an electron acceptor during anaerobic respiration (Glaring et al., 2015; Lu et al., 2014). *Hydrogenophaga* was a common bacterium flora in polluted environment, and acquired their energy by denitrification (Muturi et al., 2017; Park et al., 2005). Therefore, nitrate concentration was an important factor regulating community structure change. *Phyllobacteriaceae*

has a remarkable adaptive capacity to the environment (Jurado et al., 2005; Liu et al., 2012). In addition to its potential for denitrification, it might also be produced in the carbon cycle. *Mycobacterium* was distributed in many habitats (Liu et al., 2017) and closely related to carbon decomposition. *Flavobacteriales* and *Novosphingobium* were also common taxa in contaminated habitats (Jiao et al., 2016; Salis et al., 2017) and they could produce transparent exopolymer particles (Taylor et al., 2014; Xing et al., 2015) to reduce the toxicity of heavy metals. The highest relative abundance of *Legionella* was in SUSW (Fig. 4) and majority of *Legionella* species were of aquatic origin and were considered as facultative pathogenic (Burstein et al., 2016; Lesnik et al., 2016). In addition, Wullings (Wullings et al., 2011) described that the abundance and diversity of *Legionella* were influenced by the dissolved organic carbon in drinking water, but whether they had same adaptability in AlkMD is still not reported.

4.3. Change in copy number of denitrifying genes and availability of energy

Nitrate concentrations were an important factor affecting the change of denitrifying functional gene abundances following the nitrate gradient in the water column as previously observed in the Colne estuary (Smith et al., 2015), the boreal lakes (Saarenheimo et al., 2015) and groundwater (Zhang et al., 2016). Available energy directly influences bacterial cellular metabolism and was related to chemical processes such as nutrient availability (Siles and Margesin, 2016). Denitrification is driven by denitrifying microorganisms and is crucial in the biogeochemical cycle of nitrogen. Our results showed that denitrifying bacterial abundance and relative abundance could change drastically in conjunction with environmental variation (Table 4, Fig. 8).

The consistent increase of *nirS* from STW1 to SDSW (Fig. 6) was mainly due to the inhibition effect of Pb and Zn gradually decreased along the flow direction of tailings water (Table 4), indicating that denitrifying bacteria were highly sensitive to heavy metal contamination (Dell'Anno et al., 2003). The copy numbers of *nirK* and *nosZ_I* were significantly correlated with the NO_3^- and NO_2^- , but they showed an opposite trend (Table 4). It showed that they had different ecological adaptabilities (Coyotzi et al., 2017). The relative abundances of the three denitrifying genes were significantly correlated with the nutrition gradient (sampling position) (Table 4, Fig. 8), which was consistent with other studies (Franklin et al., 2017; Saarenheimo et al., 2015). The decrease of NO_3^- and NO_2^- concentration reduced the abundance of denitrifying bacteria. The total *nirS*+*nirK*/*nosZ_I* ratio was below 1:1 in this study, indicating that the microbial community had a higher potential to reduce N_2O than to produce it. This implies that there won't be much greenhouse gas (N_2O) emissions into the atmosphere during the denitrification process.

Moreover, we found that both abundance and relative abundance of *nirS* and *nirK* were minimal in SUSW and this might be due to the higher Zn but lower Cu concentration. Bioavailability of Cu and Fe could control the expression and activity of nitrite and nitrous oxide reductases. While the production of *nirS* gene was an iron containing cd1-type reductase and that of *nirK* was a copper-containing reductases. Possible Cu and Fe limitation might lead to decrease in abundance of *nirS* and *nirK*. Unfortunately, data on Fe concentrations were not available, and we could not fully exclude Fe limitation as a controlling factor in abundance of *nirS* decrease in SUSW. The variation trend of abundance and relative abundance of *nosZ_I* gene was different from that of *nirS* and *nirK*, and the

abundance of *nosZ_I* was the lowest (Fig. 6), but its relative abundance was the highest in STW1 (Fig. 7), which closely related to the abundance of *Acinetobacter* (Fig. 4d). *Acinetobacter* was a main denitrifying bacterium that containing the *nosZ_I* gene. In order to adapt these harsh environments, *Acinetobacter* have developed compatible functions such as nitrogen metabolism (Coyotzi et al., 2017) and heavy metals tolerance (Abdelhaleem et al., 2006).

5. Conclusions

In summary, the results showed that compositional variation of bacteria was related to water chemistry variables in this study area, further implying the influence of environment changes on community assembly. Bacterial community composition was strongly controlled by the availability of nutrients like carbon, nitrogen, sulfur and the toxic effects of heavy metals, suggesting the importance of niche-based processes in microbial community assembly may strongly depend on the local environmental context. Bacterial abundance and diversity were influenced by EC, NO_3^- , NO_2^- , and SO_4^{2-} . The abundances of core taxa including class, order, family and genus were significantly correlated with nitrogen (NO_3^- and NO_2^-) content. Moreover core taxa in class, order and family level were shaped by the SO_4^{2-} and pH. The changes of NO_3^- and NO_2^- influenced the abundances of *nirK* and *nosZ_I* rather than *nirS* and the latter might be related to TOC. Heavy metals (As, Pb and Zn) significantly reduced the abundances of all bacteria and denitrifying bacteria while Cu promoted the abundance of denitrifying bacteria. Our results thus highlighted that species-sorting processes force drove community structure and functionally similar taxa in this highly polluted ecosystem. A better understanding of the adaptation mechanisms of microbial communities in AlkMD is needed to predict how environmental alteration is likely to affect microbial communities.

Acknowledgments

This study was supported by National Science Foundation of China (31772450; 31600308) and the grants of the Shanxi Scientific and Technological project (No.20150313001-3).

Appendix A. Supplementary data

Supplementary data related to this article can be found at <https://doi.org/10.1016/j.watres.2018.01.014>.

References

- Abdelhaleem, D., Zaki, S., Abulhamd, A., Elbery, H., Abu-Elreesh, G., 2006. *Acinetobacter* bioreporter assessing heavy metals toxicity. J. Basic Microbiol. 46 (5), 339–347.
- Ai, C., Liang, G.Q., Wang, X.B., Sun, J.W., He, P., Zhou, W., 2017. A distinctive root-inhabiting denitrifying community with high $\text{N}_2\text{O}/(\text{N}_2\text{O}+\text{N}_2)$ product ratio. Soil Biol. Biochem. 109, 118–123.
- Allison, S.D., Lu, Y., Weihe, C., Goulden, M.L., Martiny, A.C., Treseder, K.K., Martiny, J.B.H., 2013. Microbial abundance and composition influence litter decomposition response to environmental change. Ecology 94 (3), 714–725.
- Baeseman, J.L., Smith, R.L., Silverstein, J., 2006. Denitrification potential in stream sediments impacted by acid mine drainage: effects of pH, various electron donors, and iron. Microb. Ecol. 51 (2), 232–241.
- Berlemont, R., Allison, S.D., Weihe, C., Lu, Y., Brodie, E.L., Martiny, J.B.H., Martiny, A.C., 2014. Cellulolytic potential under environmental changes in microbial communities from grassland litter. Front. Microbiol. 5, 1–10.
- Bier, R.L., Voss, K.A., Bernhardt, E.S., 2015. Bacterial community responses to a gradient of alkaline mountaintop mine drainage in Central Appalachian streams. ISME J. 9 (6), 1378–1390.
- Burstein, D., Amaro, F., Zusman, T., Lifshitz, Z., Cohen, O., Gilbert, J.A., Pupko, T., Shuman, H.A., Segal, G., 2016. Genomic analysis of 38 *Legionella* species identifies large and diverse effector repertoires. Nat. Genet. 48 (2), 167–175.

- Carlisle, D.M., Clements, W.H., 2005. Leaf litter breakdown, microbial respiration and shredder production in metal-polluted streams. *Freshw. Biol.* 50 (2), 380–390.
- Castelle, C.J., Brown, C.T., Thomas, B.C., Williams, K.H., Banfield, J.F., 2017. Unusual respiratory capacity and nitrogen metabolism in a paracubacterium (OD1) of the candidate phyla radiation. *Sci. Rep.* 7, 1–12.
- Chan, Y., Van Nostrand, J.D., Zhou, J.Z., Pointing, S.B., Farrell, R.L., 2013. Functional ecology of an antarctic dry valley. *P. Natl Acad. Sci. USA* 110 (22), 8990–8995.
- Coyotzi, S., Doxey, A.C., Clark, I.D., Lapen, D.R., Van Cappellen, P., Neufeld, J.D., 2017. Agricultural soil denitrifiers possess extensive nitrite reductase gene diversity. *Environ. Microbiol.* 19 (3), 1189–1208.
- Crump, B.C., Amaral-Zettler, L.A., Kling, G.W., 2012. Microbial diversity in arctic freshwaters is structured by inoculation of microbes from soils. *ISME J.* 6 (9), 1629–1639.
- Dell'Anno, A., Mei, M.L., Ianni, C., Danovaro, R., 2003. Impact of bioavailable heavy metals on bacterial activities in coastal marine sediments. *World J. Microbiol. Biotechnol.* 19 (1), 93–100.
- Dini-Andreote, F., de Cássia Pereira E Silva, M., Triado-Margarit, X., Casamayor, E.O., van Elsas, J.D., Salles, J.F., 2014. Dynamics of bacterial community succession in a salt marsh chronosequence: evidences for temporal niche partitioning. *ISME J.* 8 (10), 1989–2001.
- Fan, M.C., Lin, Y.B., Huo, H.B., Liu, Y., Zhao, L., Wang, E.T., Chen, W.M., Wei, G.H., 2016. Microbial communities in riparian soils of a settling pond for mine drainage treatment. *Water Res.* 96, 198–207.
- Flemming, Hans-Curt, Wingender, J., 2010. The biofilm matrix. *Nat. Rev. Microbiol.* 8 (9), 623–633.
- Franklin, R.B., Morrissey, E.M., Morina, J.C., 2017. Changes in abundance and community structure of nitrate-reducing bacteria along a salinity gradient in tidal wetlands. *Pedobiologia* 60, 21–26.
- Freitas, S., Hatosy, S., Fuhrman, J.A., Huse, S.M., Welch, D.B.M., Sogin, M.L., Martiny, A.C., 2012. Global distribution and diversity of marine *Verrucomicrobia*. *ISME J.* 6 (8), 1499–1505.
- Glaring, M.A., Vester, J.K., Lylloff, J.E., Abu Al-Soud, W., Sørensen, S.J., Stougaard, P., 2015. Microbial diversity in a permanently cold and alkaline environment in Greenland. *PLoS One* 10 (4), 1–22.
- Gonzalez-Martinez, A., Rodriguez-Sanchez, A., Rodelas, B., Abbas, B.A., Martinez-Toledo, M.V., van Loosdrecht, M.C.M., Osorio, F., Gonzalez-Lopez, J., 2015. 454-Pyrosequencing analysis of bacterial communities from autotrophic nitrogen removal bioreactors utilizing universal primers: effect of annealing temperature. *Biomed. Res. Int* 2015 (2–3), 1–12.
- Gülay, A., Musovic, S., Albrechtsen, H., Al-Soud, W.A., Sørensen, S.J., Smets, B.F., 2016. Ecological patterns, diversity and core taxa of microbial communities in groundwater-fed rapid gravity filters. *ISME J.* 10 (9), 1–14.
- Guo, G.X., Kong, W.D., Liu, J.B., Zhao, J.X., Du, H.D., Zhang, X.Z., Xia, P.H., 2015. Diversity and distribution of autotrophic microbial community along environmental gradients in grassland soils on the Tibetan Plateau. *Appl. Microbiol. Biot* 99 (20), 8765–8776.
- Harter, J., Krause, H.M., Schuettler, S., Ruser, R., Fromme, M., Scholten, T., Kappler, A., Behrens, S., 2014. Linking N₂O emissions from biochar-amended soil to the structure and function of the N-cycling microbial community. *ISME J.* 8 (3), 660–674.
- He, Z.G., Xie, X.H., Xiao, S.M., Liu, J.S., Qiu, G.Z., 2007. Microbial diversity of mine water at Zhong Tiaoshan copper mine, China. *J. Basic Microbiol.* 47 (6), 485–495.
- Hou, J.Q., Li, M.X., Mao, X.H., Hao, Y., Ding, J., Liu, D.M., Xi, B.D., Liu, H.L., 2017. Response of microbial community of organic-matter-impoverished arable soil to long-term application of soil conditioner derived from dynamic rapid fermentation of food waste. *PLoS One* 12 (4), 1–15.
- Hou, S.B., Makarova, K.S., Saw, J.H., Senin, P., Ly, B.V., Zhou, Z.M., Ren, Y., Wang, J.M., Galperin, M.Y., Omelchenko, M.V., Wolf, Y.I., Yutin, N., Koonin, E.V., Stott, M.B., Mountain, B.W., Crowe, M.A., Smirnova, A.V., Dunfield, P.F., Feng, L., Wang, L., Alam, M., 2008. Complete genome sequence of the extremely acidophilic methanotroph isolate V4, *Methylacidiphilum infernorum*, a representative of the bacterial phylum *Verrucomicrobia*. *Biol. Direct* 3 (1), 1–25.
- Huang, L., Kuang, J., Shu, W., 2016. Microbial ecology and evolution in the acid mine drainage model system. *Trends Microbiol.* 24 (7), 581–593.
- Ishii, S., Ohno, H., Tsuboi, M., Otsuka, S., Senoo, K., 2011. Identification and isolation of active N₂O reducers in rice paddy soil. *ISME J.* 5 (12), 1936–1945.
- Jiao, S., Chen, W.M., Wang, E.T., Wang, J.M., Liu, Z.S., Li, Y.N., Wei, G.H., 2016. Microbial succession in response to pollutants in batch-enrichment culture. *Sci. Rep.* 6, 1–11.
- Jurado, V., Laiz, L., Gonzalez, J.M., Hernandez-Marine, M., Valens, M., Saiz-Jimenez, C., 2005. *Phyllobacterium catacumbae* sp. Nov., A member of the order 'Rhizobiales' isolated from Roman catacombs. *Int. J. Syst. Evol. Microbiol.* 55 (4), 1487–1490.
- Kuang, J.L., Huang, L.N., He, Z.L., Chen, L.X., Hua, Z.S., Pu, J., Li, S.J., Liu, J., Li, J.T., Zhou, J.Z., Shu, W.S., 2016. Predicting taxonomic and functional structure of microbial communities in acid mine drainage. *ISME J.* 10 (6), 1527–1539.
- Kumari, D., Pan, X.L., Achal, V., Zhang, D.Y., Al-Misned, F.A., Mortuza, M.G., 2015. Multiple metal-resistant bacteria and fungi from acidic copper mine tailings of Xinjiang, China. *Environ. Earth Sci.* 74 (4), 3113–3121.
- Lee, J.E., Buckley, H.L., Etienne, R.S., Lear, G., 2013. Both species sorting and neutral processes drive assembly of bacterial communities in aquatic microcosms. *FEMS Microbiol. Ecol.* 86 (2), 288–302.
- Lesnik, R., Brettar, I., Höfle, M.G., 2016. *Legionella* species diversity and dynamics from surface reservoir to tap water: from cold adaptation to thermophily. *ISME J.* 10 (5), 1064–1080.
- Li, Q., Hu, Q., Zhang, C., Müller, W.E.G., Schröder, H.C., Li, Z., Zhang, Y., Liu, C., Jin, Z., 2015. The effect of toxicity of heavy metals contained in tailing sands on the organic carbon metabolic activity of soil microorganisms from different land use types in the karst region. *Environ. Earth Sci.* 74 (9), 6747–6756.
- Liu, J.X., Li, C., Jing, J.H., Jia, T., Liu, X.G., Wang, X.Y., Chai, B.F., 2017. Composition and environmental adaptation of microbial community in shibahe copper tailing in Zhongtiao mountain in Shanxi. *Environ. Sci.* 38 (1), 320–328.
- Liu, M., Lu, F., Zhong, L., Kjelleberg, S., Thomas, T., 2012. Metaproteomic analysis of a community of sponge symbionts. *ISME J.* 6 (8), 1515–1525.
- Lu, H.J., Chandran, K., Stensel, D., 2014. Microbial ecology of denitrification in biological wastewater treatment. *Water Res.* 64, 237–254.
- Muturi, E.J., Donthu, R.K., Fields, C.J., Moise, I.K., Kim, C., 2017. Effect of pesticides on microbial communities in container aquatic habitats. *Sci. Rep.* 7, 1–10.
- Mykrä, H., Tolkkinen, M., Heino, J., 2017. Environmental degradation results in contrasting changes in the assembly processes of stream bacterial and fungal communities. *Oikos* 126 (9), 1291–1298.
- Nie, Y., Zhao, J.Y., Tang, Y.Q., Guo, P., Yang, Y.F., Wu, X.L., Zhao, F.Q., 2016. Species divergence vs. Functional convergence characterizes crude oil microbial community assembly. *Front. Microbiol.* 7, 1254.
- Niyogi, D.K., Koren, M., Arbuckle, C.J., Townsend, C.R., 2007. Stream communities along a catchment land-use gradient: subsidy-stress responses to pastoral development. *Environ. Manage.* 39 (2), 213–225.
- Pan, H., Li, Y., Guan, X.M., Li, J.Y., Xu, X.Y., Liu, J., Zhang, Q.C., Xu, J.M., Di, H.J., 2016. Management practices have a major impact on nitrifier and denitrifier communities in a semiarid grassland ecosystem. *J. Soils Sediments* 16 (3), 896–908.
- Park, H.L., Choi, Y., Pak, D., 2005. Autohydrogenotrophic denitrifying microbial community in a glass beads biofilm reactor. *Biotechnol. Lett.* 27 (13), 949–953.
- Roguet, A., Laigle, G.S., Therial, C., Bressy, A., Soullignac, F., Catherine, A., Lacroix, G., Jardillier, L., Bonhomme, C., Lerch, T.Z., Lucas, F.S., 2015. Neutral community model explains the bacterial community assembly in freshwater lakes. *FEMS Microbiol. Ecol.* 91 (11), 1–11.
- Saarenheimo, J., Tirola, M.A., Rissanen, A.J., 2015. Functional gene pyrosequencing reveals core proteobacterial denitrifiers in boreal lakes. *Front. Microbiol.* 6, 1–12.
- Salis, R.K., Bruder, A., Piggott, J.J., Summerfeld, T.C., Matthaei, C.D., 2017. High-throughput amplicon sequencing and stream benthic bacteria: identifying the best taxonomic level for multiple-stressor research. *Sci. Rep.* 7, 1–12.
- Schneider, A.R., Gommeaux, M., Duclercq, J., Fanin, N., Conreux, A., Alahmad, A., Lacoux, J., Roger, D., Spicher, F., Ponthieu, M., Cancès, B., Morvan, X., Marin, B., 2017. Response of bacterial communities to Pb smelter pollution in contrasting soils. *Sci. Total Environ.* 605–606, 436–444.
- Shen, C.C., Ge, Y., Yang, T., Chu, H.Y., 2017. Verrucomicrobial elevational distribution was strongly influenced by soil pH and carbon/nitrogen ratio. *J. Soils Sediments* 17 (10), 2449–2456.
- Siles, J.A., Margesin, R., 2016. Abundance and diversity of bacterial, archaeal, and fungal communities along an altitudinal gradient in alpine forest soils: what are the driving factors? *Microb. Ecol.* 72 (1), 207–220.
- Smith, C.J., Dong, L.F., Wilson, J., Stott, A., Osborn, A.M., Nedwell, D.B., 2015. Seasonal variation in denitrification and dissimilatory nitrate reduction to ammonia process rates and corresponding key functional genes along an estuarine nitrate gradient. *Front. Microbiol.* 6, 1–11.
- Sun, W.M., Xiao, E.Z., Wang, Y., Dong, Y.R., Xiao, T.F., Ning, Z.P., Chen, H.Y., Xiao, Q.X., 2016. Characterization of the microbial community composition and the distribution of Fe-metabolizing bacteria in a creek contaminated by acid mine drainage. *App. Microbiol. Biot* 100 (19), 1–13.
- Taylor, J.D., Cottingham, S.D., Billinge, J., Cunliffe, M., 2014. Seasonal microbial community dynamics correlate with phytoplankton-derived polysaccharides in surface coastal waters. *ISME J.* 8 (1), 245–248.
- Trivedi, P., Anderson, I.C., Singh, B.K., 2013. Microbial modulators of soil carbon storage: integrating genomic and metabolic knowledge for global prediction. *Trends Microbiol.* 21 (12), 641–651.
- Wrighton, K.C., Thomas, B.C., Sharon, I., Miller, C.S., Castelle, C.J., VerBerkmoes, N.C., Wilkins, M.J., Hettich, R.L., Lipton, M.S., Williams, K.H., Long, P.E., Banfield, J.F., 2012. Fermentation, hydrogen, and sulfur metabolism in multiple uncultivated bacterial phyla. *Science* 337 (80), 1661–1665.
- Wullings, B.A., Bakker, G., van der Kooij, D., 2011. Concentration and diversity of uncultured *Legionella* spp. in two unchlorinated drinking water supplies with different concentrations of natural organic matter. *Appl. Environ. Microbiol.* 77 (2), 634–641.
- Xing, P., Hahnke, R.L., Unfried, F., Markert, S., Huang, S.X., Barbeyron, T., Harder, J., Becher, D., Schweder, T., Kcner, F.O.G., Amann, R.L., Teeling, H., 2015. Niches of two polysaccharide-degrading *Polaribacter* isolates from the North Sea during a spring diatom bloom. *ISME J.* 9 (6), 1410–1422.
- Xing, W., Li, J.L., Li, P., Wang, C., Cao, Y.N., Li, D.S., Yang, Y.F., Zhou, J.Z., Zuo, J.N., 2017. Effects of residual organics in municipal wastewater on hydrogenotrophic denitrifying microbial communities. *J. Environ. Sci.* 3, 1–9.
- Xu, M.Y., Wu, W.M., Wu, L.Y., He, Z.L., Van Nostrand, J.D., Deng, Y., Luo, J., Carley, J.,

- Ginder-Vogel, M., Gentry, T.J., Gu, B., Watson, D., Jardine, P.M., Marsh, T.L., Tiedje, J.M., Hazen, T., Criddle, C.S., Zhou, J.Z., 2010. Responses of microbial community functional structures to pilot-scale uranium *in situ* bioremediation. *ISME J.* 4 (8), 1060–1070.
- Yadav, S., Prajapati, R., Atri, N., 2016. Effects of UV-B and heavy metals on nitrogen and phosphorus metabolism in three cyanobacteria. *J. Basic Microbiol.* 56 (1), 2–13.
- Zhang, Y., Ji, G.D., Wang, R.J., 2016. Functional gene groups controlling nitrogen transformation rates in a groundwater- restoring denitrification biofilter under hydraulic retention time constraints. *Ecol. Eng.* 87, 45–52.
- Zhou, J.Z., Deng, Y., Shen, L., Wen, C.Q., Yan, Q.Y., Ning, D., Qin, Y.J., Xue, K., Wu, L.Y., He, Z.L., Voordeckers, J.W., Van Nostrand, J.D., Buzzard, V., Michaletz, S.T., Enquist, B.J., Weiser, M.D., Kaspari, M., Waide, R., Yang, Y.F., Brown, J.H., 2016. Temperature mediates continental-scale diversity of microbes in forest soils. *Nat. Comms* 7, 1–10.